Supporting Information

A cationic lipid with advanced membrane fusion performance for pDNA and mRNA delivery

Yu Wei[a, ‡], Ting He[a, ‡], Qunjie Bi[a], Huan Yang[a], Xueyi Hu[a], Rongrong Jin[a], Hong Liang[b, c], Yongqun Zhu[d], Rongsheng Tong[b, c*], and Yu Nie[a*]*

[a] National Engineering Research Center for Biomaterials/College of Biomedical Engineering, Sichuan University, Chengdu 610064, China

[b] Department of Pharmacy, Sichuan Academy of Medical Sciences & Sichuan Provincial People's Hospital, School of Medicine, University of Electronic Science and Technology of China, Chengdu 610072, China.

[c] Personalized Drug Therapy Key Laboratory of Sichuan Province, School of Medicine, University of Electronic Science and Technology of China, Chengdu 610072, China.

[d] Life Sciences Institute and Innovation Center for Cell Signaling Network, Zhejiang University, Hangzhou 310058, China.

‡ Equal contribution to the manuscript as co-first authors

* E-mail: nie_yu@scu.edu.cn; lianghong3689@163.com; 2207132448@qq.com

Fax: +86-28-8541-0246; Tel: +86-28-8541-284

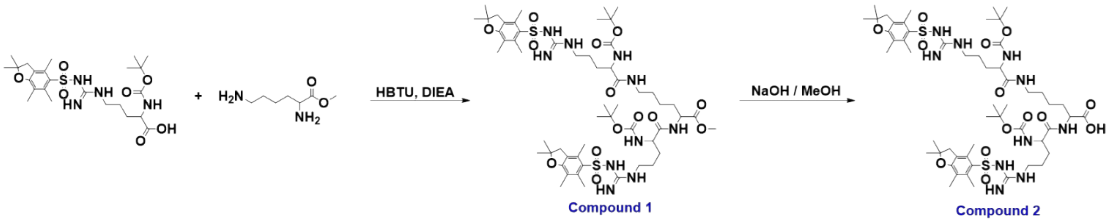

Figure S1. Synthesis of the arginine-containing cationic segment.

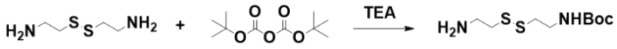

Figure S2. Synthesis of the linker with a disulfide bond.

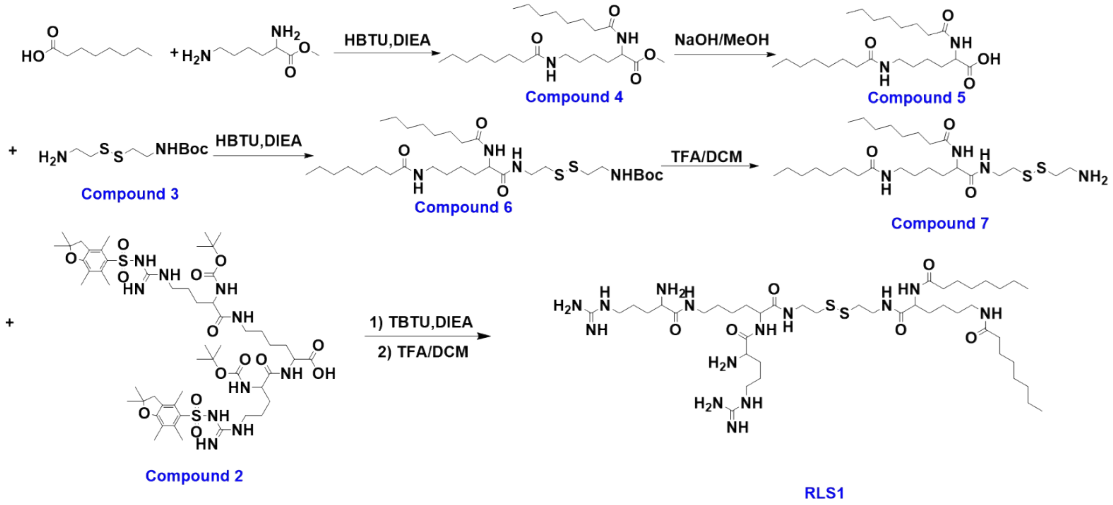

Figure S3. Synthesis of cationic lipid RLS1.

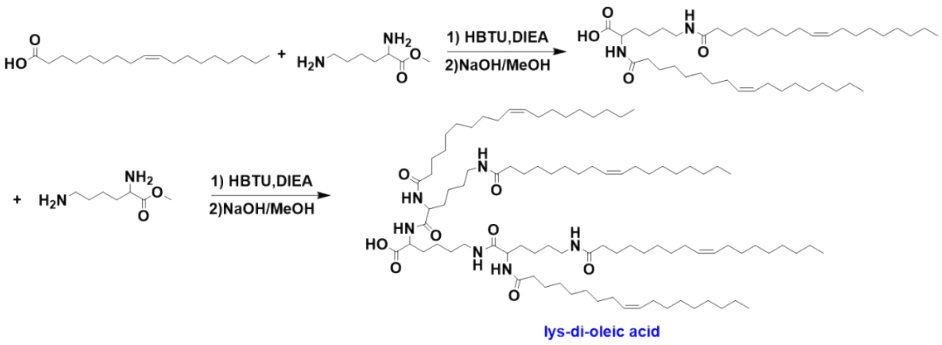

Figure S4. Synthesis of lys-di-oleic acid

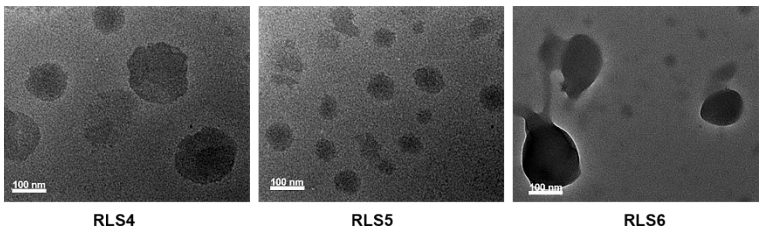

Figure S5. Transmission electron microscope (TEM) images of RLS4 (126.4 nm), RLS5 (90.6 nm), and RLS6 (148.1 nm) lipid assemblies. The scale bar was 100 nm.

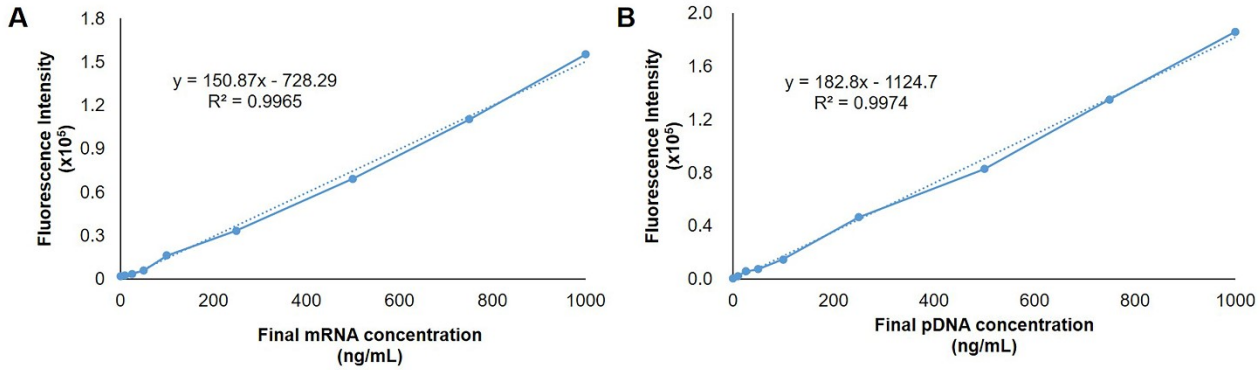

Figure S6. The standard curve of mRNA (A) and pDNA (B) by RiboGreen and PicoGreen staining, respectively.

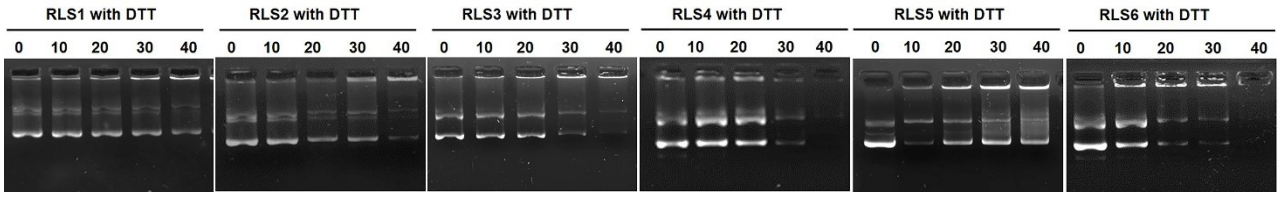

Figure S7. Gel retardation assay of cationic assemblies/pDNA complexes at different N/P ratios in the presence of 10 mmol/L DTT.

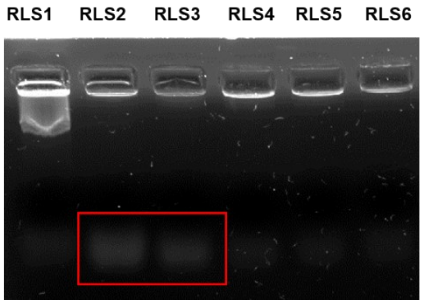

Figure S8. Six lipoplexes stability in 10% FBS by gel electrophoresis assays.

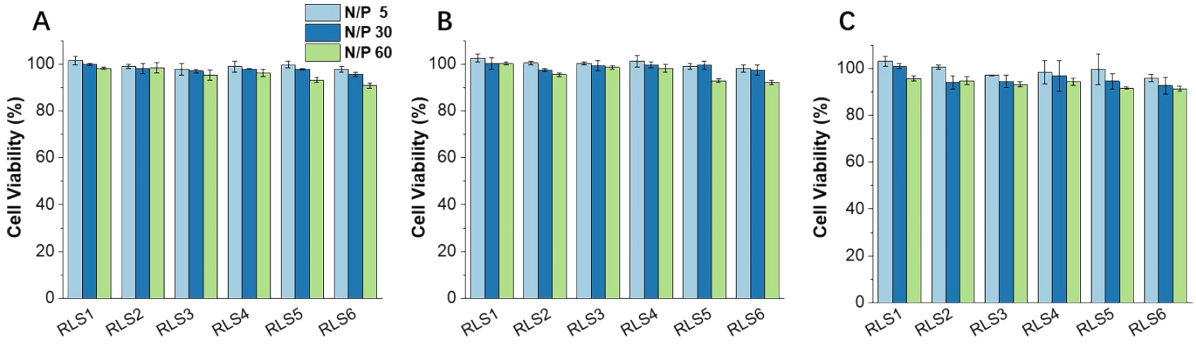

Figure S9. The cell viability with 10% FBS of different nanoparticles in HEK293 (A), HepG2 cells (B), and Hela cells (C).

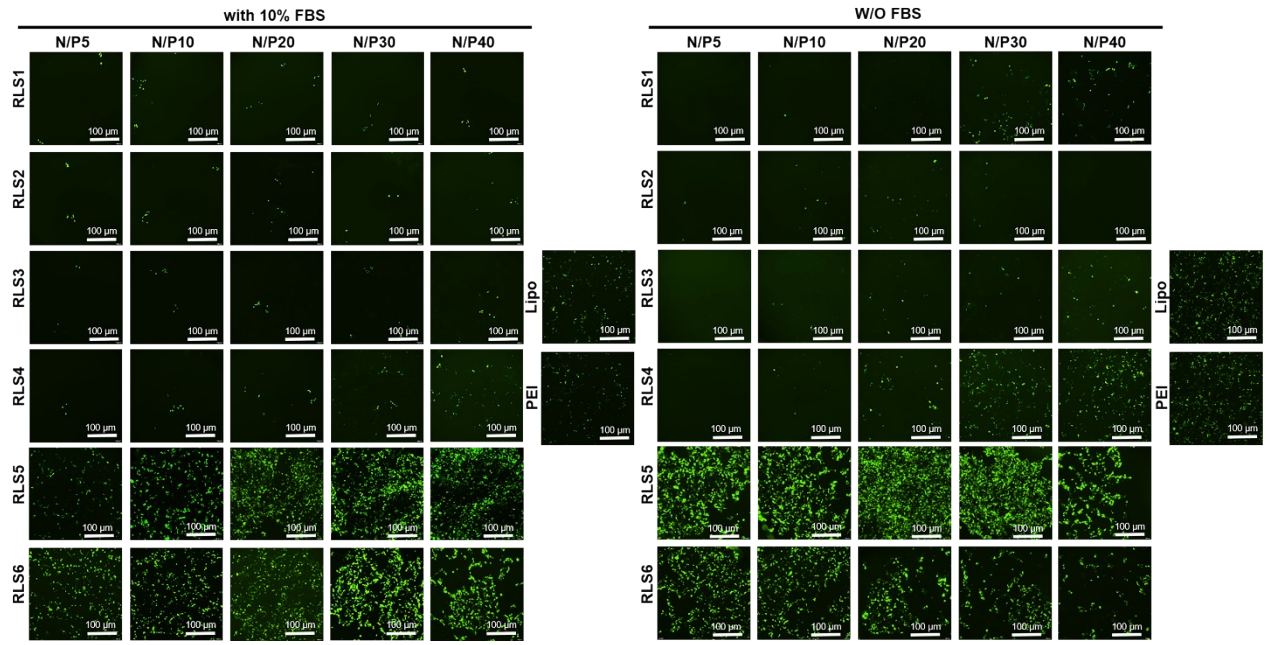

Figure S10. Fluorescence microscopy images of cells with pEGFP transfection on HEK-293 cells (W/O: without).

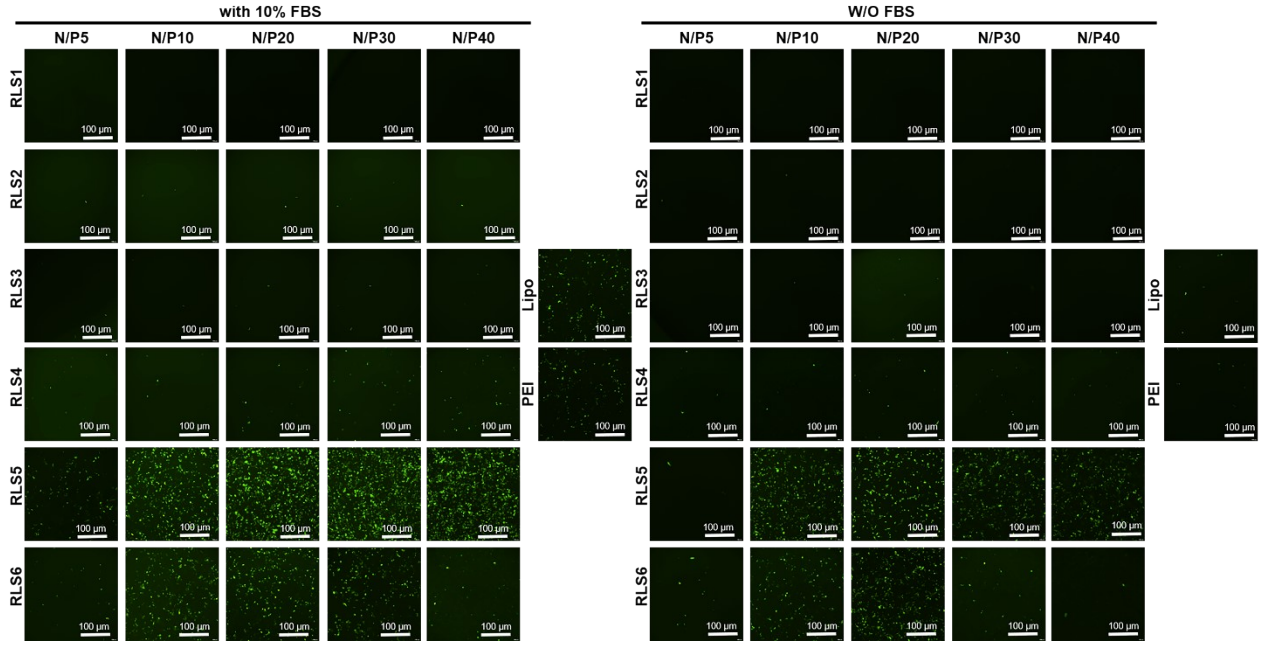

Figure S11. Fluorescence microscopy images of cells with pEGFP transfection on HepG2 cells.

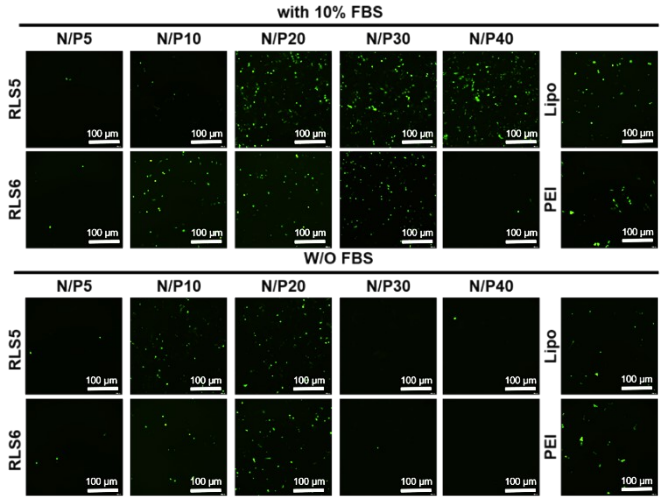

Figure S12. Fluorescence microscopy images of cells with pEGFP transfection on Hela cells.

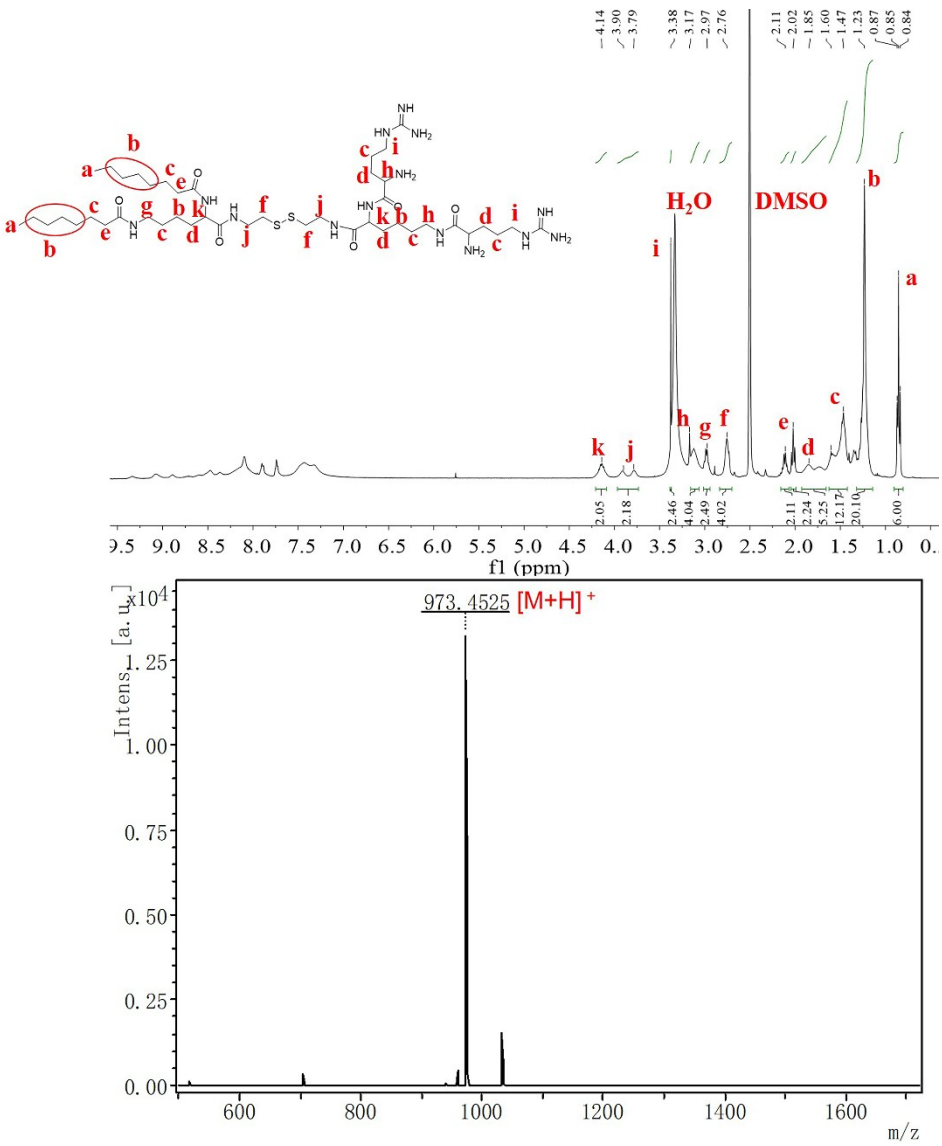

Figure S13. (A) ^{1}H-NMR of RLS1. (B) MOLDI-TOF-MS of RLS1

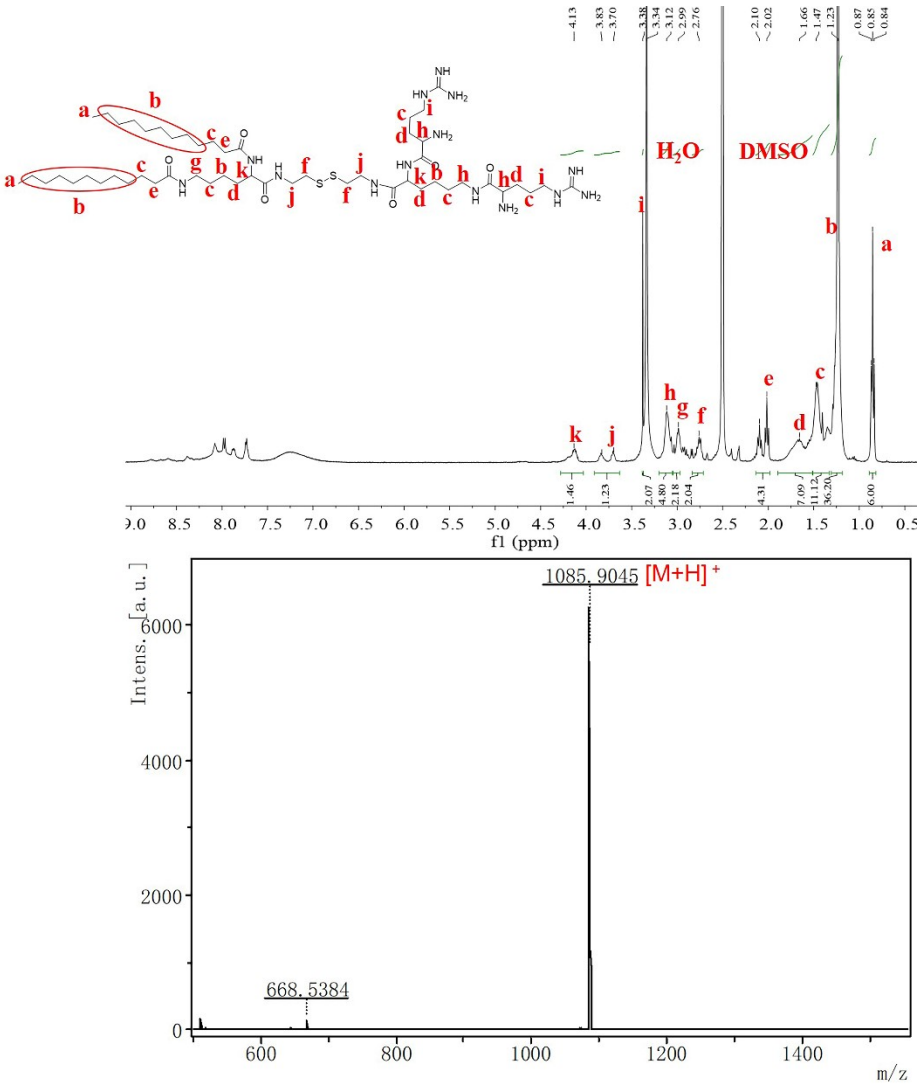

Figure S14. (A) ^{1}H-NMR of RLS2. (B) MOLDI-TOF-MS of RLS2.

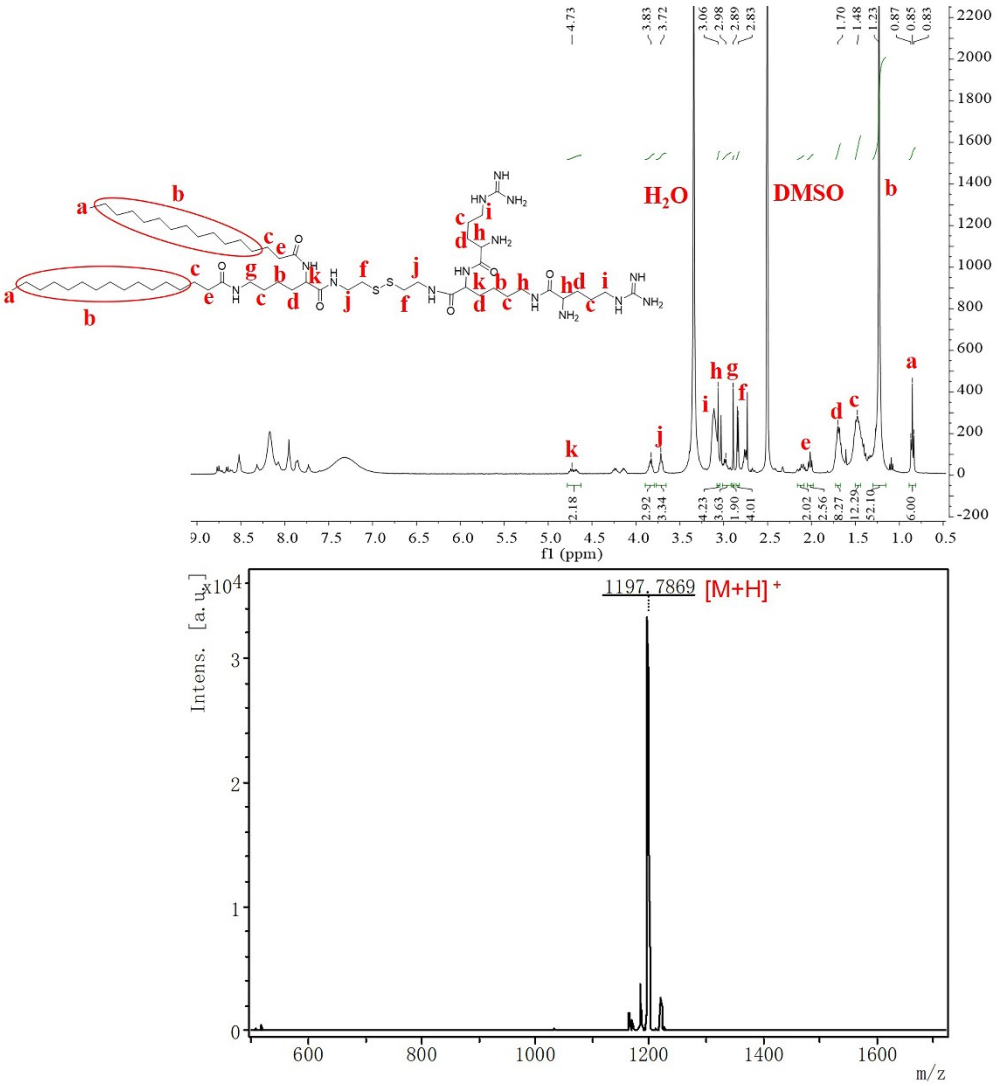

Figure S15. (A) ^{1}H-NMR of RLS3. (B) MOLDI-TOF-MS of RLS3.

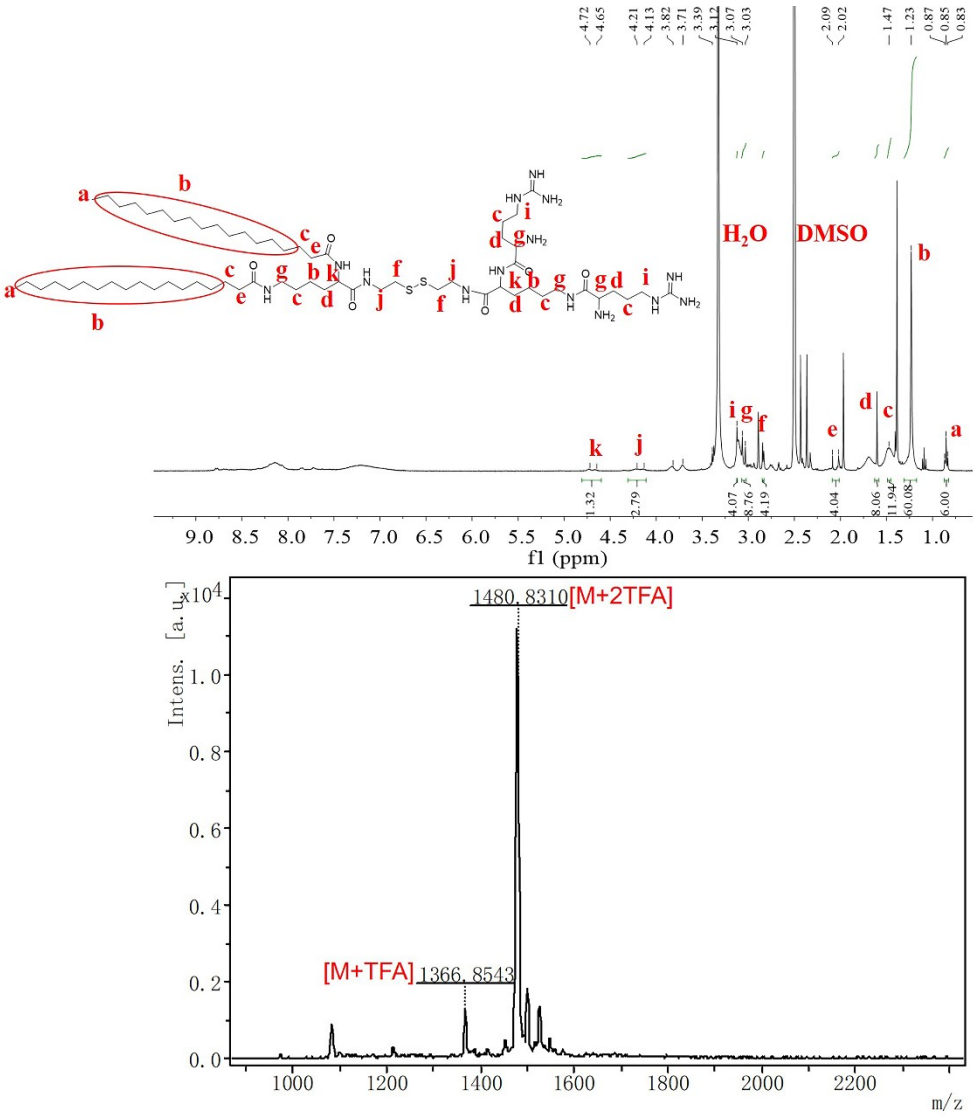

Figure S16. (A) ^{1}H-NMR of RLS4. (B) MOLDI-TOF-MS of RLS4.

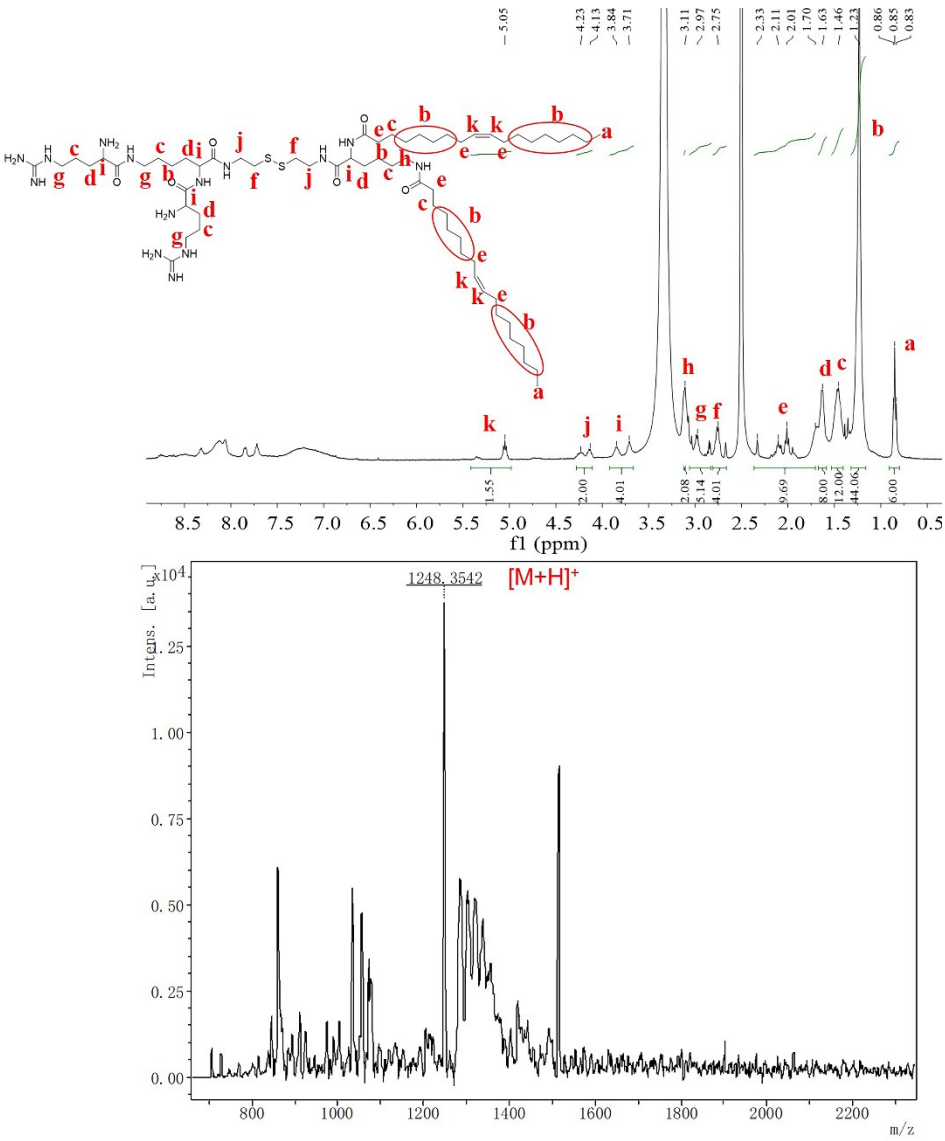

Figure S17. (A) ^{1}H-NMR of RLS5. (B) MOLDI-TOF-MS of RLS5.

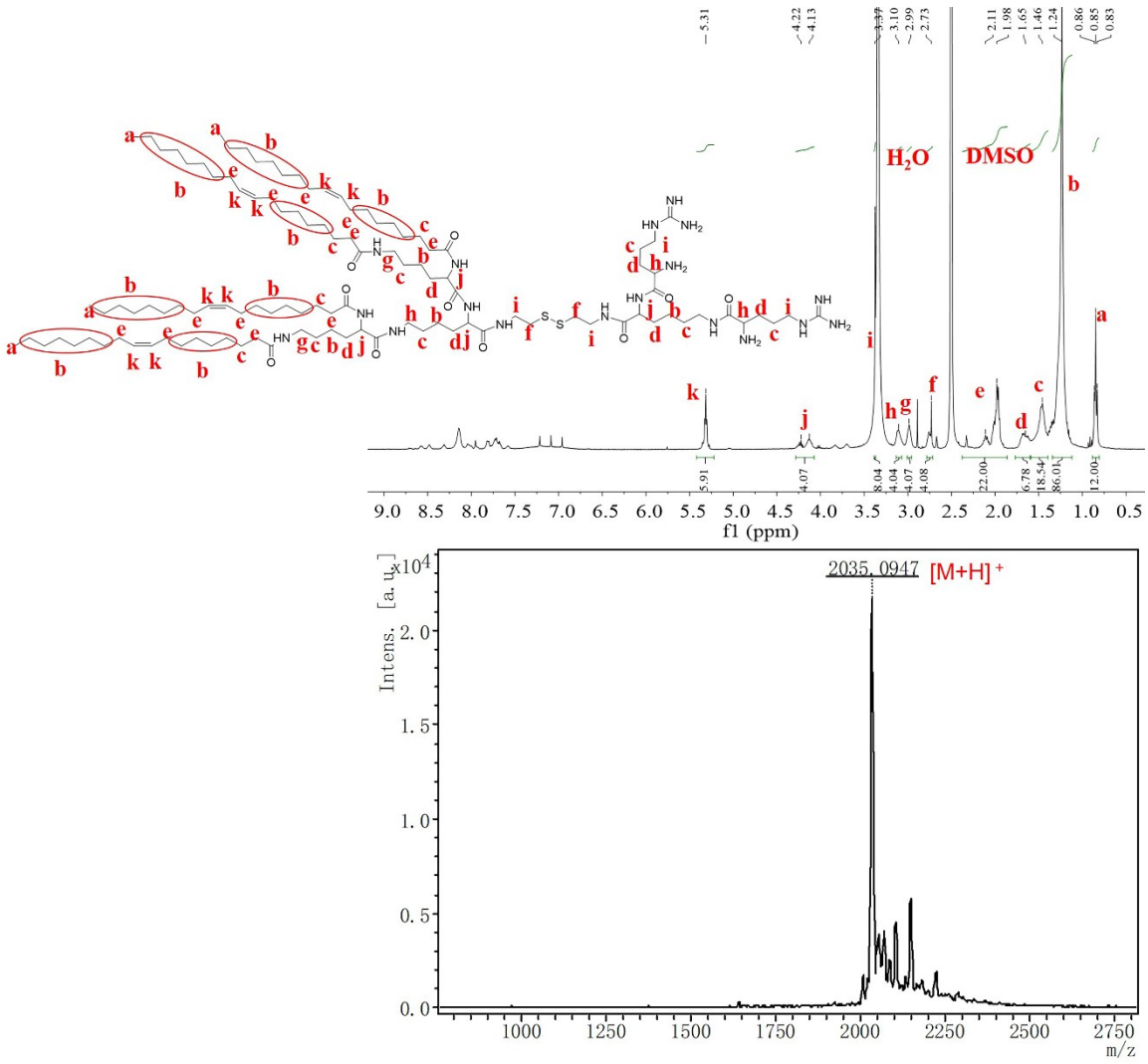

Figure S18. (A) ^{1}H-NMR of RLS6. (B) MOLDI-TOF-MS of RLS6.

Table S1. The particle size, PDI, and ζ potential of six lipid assemblies.

	Particle size (nm)	PDI	Zeta potential (mV)
RLS1	140.3 ± 21.2	0.22 ± 0.02	22.2 ± 3.7
RLS2	164.6 ± 6.8	0.24 ± 0.04	24.1 ± 2.8
RLS3	187.7 ± 12.5	0.20 ± 0.01	24.7 ± 6.1
RLS4	212.2 ± 14.6	0.28 ± 0.04	25.5 ± 3.2
RLS5	154.3 ± 17.2	0.19 ± 0.03	26.0 ± 2.9
RLS6	220.2 ± 5.2	0.27 ± 0.06	27.1 ± 3.9

Table S2. The encapsulation efficiency of RLS5/mRNA and RLS1-6/pDNA.

	N/P	Loaded gene	Total gene weight (ng)	Free gene weight (ng)	Encapsulation efficiency (%)
RLS5	5	mRNA	200	7.95	96.03
RLS1	20	pDNA	200	9.41	95.43
RLS2	20	pDNA	200	7.71	96.15
RLS3	20	pDNA	200	9.65	95.18
RLS4	20	pDNA	200	5.90	97.05
RLS5	20	pDNA	200	7.22	96.39
RLS6	20	pDNA	200	3.12	98.44

Table S3. The particle size of lipid gene complexes after 0, 15, 30, 45, and 60 min of incubation with 10% FBS.

	Time (min)	Particle size (nm)	PDI		Time (min)	Particle size (nm)	PDI
	0	312.4 ± 20.1	0.37 ± 0.07		0	234.2 ± 12.5	0.21 ± 0.02
	15	459.2 ± 13.5	0.58 ± 0.12		15	242.4 ± 31.9	0.13 ± 0.07
RLS1	30	791.1 ± 106.1	0.91 ± 0.09	RLS4	30	228.9 ± 19.2	0.25 ± 0.04
	45	590.9 ± 55.7	0.51 ± 0.04		45	247.6 ± 25.7	0.27 ± 0.03
	60	860.3 ± 69.6	0.72 ± 0.13		60	239.2 ± 11.4	0.24 ± 0.05
	0	224.3 ± 22.7	0.28 ± 0.03		0	198.2 ± 7.8	0.21 ± 0.05
	15	327.6 ± 47.3	0.53 ± 0.09		15	201.5 ± 13.6	0.24 ± 0.03
RLS2	30	401.5 ± 19.1	0.41 ± 0.11	RLS5	30	199.4 ± 2.3	0.18 ± 0.05
	45	499.9 ± 59.4	0.45 ± 0.21		45	206.7 ± 18.1	0.20 ± 0.06
	60	377.1 ± 20.1	0.60 ± 0.07		60	193.1 ± 12.6	0.27 ± 0.08
	0	246.1 ± 31.2	0.23 ± 0.04		0	254.7 ± 15.6	0.31 ± 0.05
	15	375.2 ± 12.0	0.48 ± 0.02		15	262.3 ± 28.3	0.28 ± 0.04
RLS3	30	267.5 ± 41.9	0.44 ± 0.10	RLS6	30	230.9 ± 12.7	0.33 ± 0.07
	45	321.6 ± 43.2	0.21 ±0.07		45	238.1 ± 8.7	0.25 ± 0.06
	60	348.9 ± 69.8	0.77 ± 0.47		60	257.9 ± 17.9	0.30 ± 0.01